Boundary-Layer Meteorol (2009) 132:415–436
DOI 10.1007/s10546-009-9410-6

ARTICLE

The Effects of Building Representation and Clustering in Large-Eddy Simulations of Flows in Urban Canopies

Elie Bou-Zeid · Jan Overney · Benedict D. Rogers · Marc B. Parlange

Received: 24 November 2008 / Accepted: 7 July 2009 / Published online: 23 July 2009

Abstract We perform large-eddy simulations of neutral atmospheric boundary-layer flow over a cluster of buildings surrounded by relatively flat terrain. The first investigated question is the effect of the level of building detail that can be included in the numerical model, a topic not yet addressed by any previous study. The simplest representation is found to give similar results to more refined representations for the mean flow, but not for turbulence. The wind direction on the other hand is found to be important for both mean and turbulent parameters. As many suburban areas are characterised by the clustering of buildings and homes into small areas separated by surfaces of lower roughness, we look at the adjustment of the atmospheric surface layer as it flows from the smoother terrain to the built-up area. This transition has unexpected impacts on the flow; mainly, a zone of global backscatter (energy transfer from the turbulent eddies to the mean flow) is found at the upstream edge of the built-up area.

Keywords Building representation · Global backscatter · Heterogeneous terrain · Surface roughness · Turbulent kinetic energy · Urban boundary layer · Urban canopy

1 Introduction

The combination of changing climate patterns and increasing urban populations will intensify the pressure on the infrastructure and the environment in urban zones and

E. Bou-Zeid (✉)
Department of Civil and Environmental Engineering, Princeton University,
C326-EQuad, Princeton, NJ 08544, USA
e-mail: ebouzeid@princeton.edu

E. Bou-Zeid · J. Overney · M. B. Parlange
School of Architecture, Civil and Environmental Engineering,
École Polytechnique Fédérale de Lausanne-EPFL, Lausanne, Switzerland

B. D. Rogers
School of Mechanical, Aerospace and Civil Engineering, University of Manchester,
P.O. Box 88, Sackville Street Building, Sackville Street, Manchester M60 1QD, UK

will continue to give rise to a complex set of problems concerning the health, safety, and comfort of urban populations.

Urban areas represent an important environment due to the high population density, the strong concentration of economic activity, and the associated land-use modification. Therefore, to address and mitigate the aforementioned problems, an improved understanding of the dynamics of this urban environment, and of its interaction with the surrounding natural systems, is required. Of particular interest are the dynamics of atmospheric flows in built-up areas and their impact on air quality, energy consumption, and urban microclimates. Research efforts concentrating on urban atmospheric dynamics are nevertheless lagging behind our needs and more efforts are required, especially in relation to the understanding of local atmospheric dynamics over cities and the development of adequate parameterisations for urban areas in large-scale numerical models (Britter and Hanna 2003; Coceal and Belcher 2004).

The basic challenge is related to the heterogeneity and complexity of urban environments combined with a lack of experimental and numerical tools appropriate for sensing and modelling the complex dynamics of urban systems, especially atmospheric flow and transport in urban canopies and flow-structure interactions (Rotach et al. 2002; Cheng and Castro 2002; Xie and Castro 2006). On the one hand, transport issues concerning pollutants, heat, and moisture are strongly coupled to the fluid dynamics within and over the urban canopy. On the other hand, flow patterns in these regions are strongly modified by the presence of the buildings and of the anthropogenic heat sources.

A related problem also concerns the lack of adequate parameterisations for the interaction of urban areas with their surroundings at larger scales. When weather and global circulation models are used, even large cities only cover the lowest part of one or a few grid cells. In such instances, the physical processes that occur within the building canopies cannot be simulated explicitly and must be parameterised. Development of good parameterisations at the city/regional scale is interconnected with improving our understanding of the neighbourhood-scale and street-scale atmospheric dynamics in urban areas.

In the past two decades, experimental urban canopy studies have been conducted quite extensively with the primary objective of improving the basic understanding of flow and transport in urban environments (Grimmond et al. 1998; Emeis 2004b; Emeis and Turk 2004; Eliasson et al. 2006; Roth et al. 2006) and with the long term aim of improving regional-scale parameterisations of urban surfaces in regional atmospheric models (Grimmond and Oke 1999; Emeis 2004a; Roulet et al. 2005; Coceal and Belcher 2004). Most of these parameterisations rely on a modified form of the Monin-Obukhov Similarity Theory (MOST, Monin and Obukhov 1954) to compute average vertical fluxes of momentum, heat, and other scalars (see review in Rotach et al. 2002). MOST is strictly applicable only over homogeneous surfaces, although it has often been used successfully to compute aggregate fluxes over heterogeneous natural terrains (Parlange and Brutsaert 1993; Avissar 1995; Brutsaert 1998; Molod et al. 2003; Bou-Zeid et al. 2004). Nevertheless, its universal applicability to aggregate fluxes over complex urban heterogeneities has been questioned by reviews of observational data (Roth 2000).

Recent studies have proposed more elaborate urban canopy parameterisations by incorporating explicit models for building drag rather than using an average surface roughness (Belcher et al. 2003). Some parameterisations also include models for the energy budget in the urban canopies (Masson 2000; Dupont and Mestayer 2006; also see comparison of four models in Roberts et al. 2006) including many realistic effects such as shadowing and radiation trapping induced by the street canyons (e.g. Harman and Belcher 2006).

However, at present it is difficult to assess these parameterisations against realistic data since experimental studies cannot provide complete spatial information and are limited to one

site, or at most a few specific sites. This limitation makes measurements of aggregate fluxes, which represent the primary product or output of urban boundary-layer parameterisations, very challenging.

In that regard, the development of accurate numerical techniques to study urban canopy flow is valuable since such techniques provide more complete datasets describing the turbulent urban wind and scalar fields, as well as aggregate fluxes at the city scale. Numerical studies can give complete spatial information and examine a very wide variety of geometries and scenarios. This in turn implies that the physics behind specific flow features and the role of coherent structures and the pressure field can be better studied.

The main challenge for numerical simulations of turbulent flows is the need to parameterize the unresolved physical processes and scales, and then rigorously validate the model. The large-eddy simulation (LES) technique now offers great potential since it minimizes the need for unresolved physics parameterization and hence usually compares better with experimental or field data than the traditional Reynolds-averaged numerical simulations (RANS), where all the scales of turbulence are parameterised (see examples of LES versus RANS comparison in Xie and Castro 2006 and Tominaga et al. 2008). The technique also has been widely used and validated in recent years for natural (Albertson et al. 2001; Lin and Glendening 2002; Bou-Zeid et al. 2005; Kumar et al. 2006; Kleissl et al. 2006) and urban (Cai 1999; Kanda et al. 2004; Calhoun et al. 2005; Xie and Li 2005; Zhang et al. 2006; Tseng et al. 2006) boundary layers.

This paper uses the code validated in Bou-Zeid et al. (2005) and Kumar et al. (2006) for flat terrain, in Yue et al. (2007a, b) for flow in porous corn canopies, and in Tseng et al. (2006) for built-up areas (see details in Sect. 2) to address an important issue concerning the use of the LES technique for urban environments: how much of the building details need to be included in the modelling domain. To the best of our knowledge, this is the first study of urban-canopy simulations sensitivity to building representation. Subsequently, we examine the effect of discontinuities in the built environment on the flow: except for the centres of medium and large cities, most built environments consist of clusters of building and houses separated by areas with other land-use types (typically with lower roughness). Nevertheless, the effects of transitions from flat/vegetated to built-up terrain, and vice versa, have not yet been adequately addressed.

In Sect. 2, the LES formulation and the numerical details of the numerical code are described. Section 3 presents four simulations with different wind directions and different levels of detail in the representation of the buildings in the numerical domain. In Sect. 4, we compute the average drag exerted by the cluster of buildings on the flow and the effective surface roughness of the buildings, exploring along the way the effect of wind direction and the level of detail in building representation on the results. Section 5 depicts the effect of the buildings on mean and turbulent velocity fields, and in Sect. 6, the adjustment of the incoming flow over the simulated building canopy is explored. The effect of the buildings on the shear production and dissipation of turbulent kinetic energy in the atmosphere is presented in Sect. 7.

The simulated area is the campus of the École Polytechnique Fédérale de Lausanne (EPFL) in Switzerland. The site was selected since it is currently the location of a series of field campaigns to test the use of distributed sensing networks (and new-generation remote sensing systems) in complex urban environments. Ultimately, the aim of the research effort is to develop new approaches and frameworks for combining sensing and modelling tools in urban areas. This paper however deals strictly with the computational modelling part. The campus is more representative of suburban areas with discontinuous clusters of low buildings than of extended large city centres with many high rise towers.

2 Numerical Simulations

The large-eddy simulation technique has emerged as a tool of choice for high Reynolds number turbulent flows in engineering systems (Piomelli 1999; Sagaut 2003), oceans (Shen and Yue 2001; Keylock et al. 2005), rivers (Bradbrook et al. 2000), and the atmosphere (Albertson and Parlange 1999a, b; Wood 2000; Bou-Zeid et al. 2004, 2007; Stoll and Porte-Agel 2006).

In the atmosphere, turbulence is mostly present in the atmospheric boundary layer (ABL), where turbulent motions span several orders of magnitude and turbulence is mainly generated by wind shear and buoyancy. The scale of the smallest turbulent motions, the Kolmogorov scale, is on the order of 10^{-3} m, while the largest scales are of the size of the boundary-layer depth ($\approx$500–2,000 m). The density of the computational grid required to capture these scales of turbulence is currently far beyond the capacities of even the largest computational efforts (see a discussion of computational costs of turbulent simulations in Celani 2007). By splitting the turbulent structures into resolved and subgrid-scale, using a filtering operation, LES reduces the density of the computational grid required to capture the large scales of the flow, making unsteady, three-dimensional simulations of high Reynolds number turbulent flows over large domains practicable.

The underlying assumption justifying this approach is that the largest eddies contain most of the energy and are responsible for most of the transport of momentum and scalars. Nonetheless, the effect of the subgrid-scale structures cannot be discarded and appears in the filtered Navier–Stokes equations as the divergence of an additional unknown, the subgrid-scale (SGS) stress tensor.

The isothermal LES equations in rotational form are solved here to ensure conservation of mass and kinetic energy of the inertial term (Orszag and Pao 1974),

$$\frac{\partial \tilde{u}_i}{\partial x_i} = 0, \tag{1a}$$

$$\frac{\partial \tilde{u}_i}{\partial t} + \tilde{u}_j \left(\frac{\partial \tilde{u}_i}{\partial x_j} - \frac{\partial \tilde{u}_j}{\partial x_i} \right) = -\frac{1}{\rho} \frac{\partial \tilde{p}^*}{\partial x_i} - \frac{\partial \tau_{ij}}{\partial x_j} + F_i, \tag{1b}$$

where the tilde ($\tilde{}$) denotes the resolved part of the variables, u_i is the fluid velocity in direction i, F_i is the mean streamwise pressure forcing, ρ is the fluid density, and τ_{ij} is the deviatoric or anisotropic part of the SGS stress tensor σ_{ij},

$$\tau_{ij} = \sigma_{ij} - \frac{1}{3}\sigma_{kk}\delta_{ij}. \tag{2}$$

We solve the equations pre-normalised with the domain-averaged friction velocity at the surface (u_*), the boundary-layer depth (H), and air density (ρ) so that resultant fields are already normalised with these parameters. Of specific importance for the subsequent analysis is the fact that the simulated velocity profiles are normalised with u_*. The forcing term with this normalization becomes $F_i = \Delta P H/\rho u_*^2 L_x = 1$, where ΔP is the mean streamwise pressure forcing and L_x is the streamwise length of the domain; this represents the balance between mean pressure forcing and surface drag at the bottom of the domain. Note that in the filtered Navier–Stokes equations, the molecular viscous term is neglected because the focus is on very high Reynolds number flows where viscosity is negligible at the resolved scales (its effect is relevant only at much smaller scales) and the wall layer is modelled (as opposed to resolving the viscous sublayer, see Pope 2000). The isotopic or hydrostatic part of the SGS stress tensor acts as a pressure and is therefore combined with the modified pressure term

$$\tilde{p}^* = \tilde{p} + (1/3)\rho\sigma_{kk} + (1/2)\rho\tilde{u}_j\tilde{u}_j. \quad (3)$$

The pressure is computed from a Poisson equation obtained by setting the divergence of the momentum equation to zero. This is equivalent to (and hence substitutes for) solving the continuity equation.

To close the system of equations, a parameterization for the subgrid-scale stress is required. The results of large-eddy simulations are quite sensitive to this parameterization especially in the vicinity of solid boundaries where the subgrid-scale fluxes are important and their physics are harder to model (see the discussion in Meneveau and Katz 2000, and an illustration in Bou-Zeid et al. 2005).

Most SGS parameterisations used in LES rely on the concept of eddy viscosity, ν_T, to relate the SGS stress (its deviatoric part) to the resolved rate of strain. The classic eddy-viscosity model proposed by Smagorinsky (1963) also uses the mixing-length concept to estimate eddy viscosity according to

$$\tau_{ij}^{smag} = -2\nu_T\tilde{S}_{ij} = -2(c_s\Delta)^2|\tilde{S}|\tilde{S}_{ij}, \quad (4)$$

where Δ is the grid scale and $\tilde{S}_{ij} = 0.5\left(\partial\tilde{u}_i/\partial x_j + \partial\tilde{u}_j/\partial x_i\right)$ is the resolved strain rate tensor. The Smagorinsky coefficient, c_s, is the only unknown and extensive research has been performed to determine its value. Lilly (1967) was the first to derive the value of c_s under homogeneous and isotropic flow conditions; subsequently, several procedures to compute the coefficient dynamically, from information about the smallest resolved scales, have been proposed starting with Germano et al. (1991). This has allowed the application of the model to realistic flows (very rarely homogeneous and isotropic), and in many ways has represented a massive advance in the field of computational fluid dynamics. Herein, we use a more refined model that takes into account the scale dependence of the model coefficients, which was ignored in Germano et al. (1991). The details of the development and formulation of this Lagrangian (Meneveau et al. 1996) scale-dependent (Porte-Agel et al. 2000; Bou-Zeid et al. 2008) dynamic SGS model and the numerical details of the code can be found in Bou-Zeid et al. (2005). In addition to the validation for urban flows presented below, the model has been thoroughly validated for ABL flows over homogeneous and heterogeneous surfaces (Bou-Zeid et al. 2004, 2005), diurnal ABL cycles (Kumar et al. 2006; Kleissl et al. 2006), and flow in plant canopies (Yue et al. 2007a, b).

The presence of buildings is simulated using the immersed boundary method (IBM) that mimics the effect of the buildings by imposing a virtual body force at each grid node inside the bluff body, such that the flow velocity within the bluff body is reduced to zero. Shear stresses are imposed at the building surfaces using a regular wall-model. Tseng et al. (2006) detail the IBM implementation for the model used here and validate it against wind-tunnel data for flow over a single cube (Lyn and Rodi 1994) and an array of cubes (Meinders and Hanjalic 1999, 2002). Detailed grid resolution and sensitivity studies were also conducted by Tseng et al. (2006) who concluded that beyond a grid resolution of about 6^3 nodes per cube, results converged and a good match with experimental data was obtained. At a resolution of about 4^3 nodes per cube, the match with experimental results was not as good, but was still representative of the basic flow dynamics, as depicted in Fig. 1 below, reproduced from Tseng et al. (2006) (note that the resolution requirements differ between codes that resolve the viscous sublayer and codes that use wall models, as we do here). Hence, we base the analysis of our results on these guidelines with a resolution of 4^3 nodes per cube being considered adequate only for a qualitative description of the flow.

The code is pseudo-spectral in the horizontal directions, requiring periodic horizontal boundary conditions. These periodic boundary conditions imply that an infinite sequence of

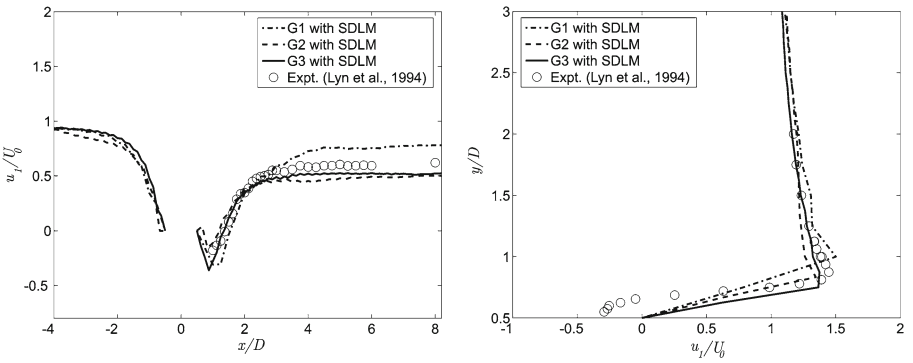

Fig. 1 Reproduced from Tseng et al. (2006), depicting the comparison of experimental data with the LES runs at different resolutions. G1 corresponds to about 4^3 nodes per cube, G2 to 6^3 and G3 to 8^3. u_1 is the mean streamwise velocity, U_0 is the free stream velocity, D is the dimension of the cube and x and y are the streamwise and vertical directions, respectively

similar domains is actually being simulated, which is not desirable in our study. To avoid this effect, an alternative inflow is generated by running a separate simulation of a neutral boundary-layer flow over a flat rough surface (roughness length $z_0 = 1$ m, representing heterogeneous areas of vegetation and houses). Successive velocity slices (y–z planes) at a fixed location in the inflow simulation are supplied as the inflow into the main simulations of urban canopy flow. These inflow conditions are imposed at the tenth y–z (axial) plane in the domain. A relaxation region is then created between the first and tenth y–z planes to smoothly adjust the velocity field from the periodic inflow (at the first plane) to the imposed inflow (at the tenth plane) and hence avoid numerical problems due to a sudden velocity adjustment in the pseudo-spectral horizontal directions (Tseng et al. 2006). The upper boundary condition is a free slip and no-penetration surface; at the lower wall and at the building walls, a no-penetration condition is again imposed and the shear stresses are computed using a local law-of-the-wall model: $\tau_{ij} = [\kappa \hat{u}_i / ln(z_j/z_0)]^2$, where κ is the von Karman constant (0.4), z_j is the perpendicular distance to the wall in the jth direction, and z_0 is the surface roughness. This formulation uses the velocity filtered at twice the grid scale ($\hat{u}_i$) to avoid the overestimation of mean domain stresses (Bou-Zeid et al. 2005). For the building walls, a roughness length $z_0 = 0.01$ m is used, while for natural surfaces not covered with buildings, $z_0 = 0.1$ m.

3 The Urban Canopy Representations

We are interested in understanding the effect of the complexity of an urban canopy representation on the results of numerical simulations of neutral atmospheric boundary-layer flow (here complexity refers to the level of detail in representing the structures of the real urban canopy in the simulation domain). The results are needed because:

- an urban canopy representation cannot possibly represent the full complexity of the real physical canopy due to computational grid resolution restrictions, and
- in most cases, the exact dimensions, location and details of every building are not readily available and are difficult to obtain.

Therefore, the following question arises: how representative are simulations over simplified versions of the real building canopy? In the following, results of large-eddy simulations of

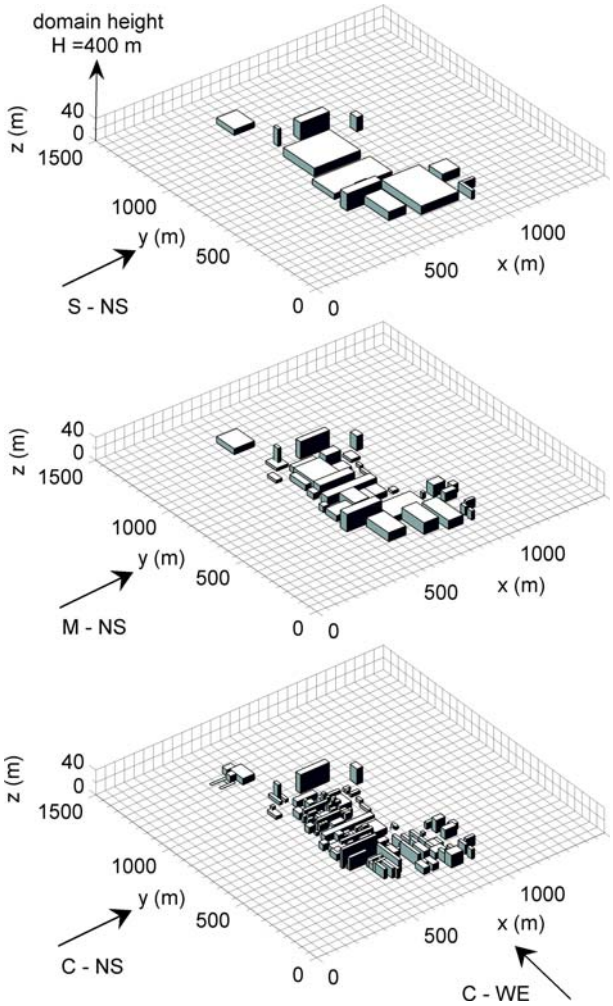

Fig. 2 The three campus representations and the directions of the simulated winds for the four simulations (the *grid* shown is not the actual numerical grid)

neutral ABL flow over different urban canopy representations of the EPFL campus for two different wind directions will be presented. The three urban canopy representations differ in the degree of detail with which they replicate the actual EFPL campus. Figure 2 depicts the three canopy representations and the acronyms of the four simulations: complex representation and west-east wind (C–WE), complex representation and north-south wind (C–NS), medium representation and north-south wind (M–NS), and simple representation and north-south wind (S–NS).

In the crudest representation, several buildings are lumped together into 12 larger blocks while the medium complexity representation comprises 37 blocks. The most complex representation of the urban canopy is composed of 127 separate blocks. Note that, while the details of the representations are significantly different, the projected surface area of the buildings, perpendicular to the streamwise direction, is about the same for the three representations.

This detail will be important later in the analysis. The surfaces in the domain that are not covered with buildings (green surface, roads, parking lots, etc.) are simply simulated as flat surfaces with a prescribed roughness height ($z_0 = 0.1$ m), as detailed in the wall model section above. The dimensions of the domain are $1{,}500 \times 1{,}500 \times 400\,\mathrm{m}^3$, and the numerical grid for all simulations comprises $100 \times 100 \times 80$ nodes. The grid spacing is hence 15 m in the two horizontal directions and 5 m in the vertical direction (starting at 2.5 m due to the staggered grid). We simulated north-south winds for all building representation levels, and west-east winds only with the complex representation. Most of the campus buildings are oriented along the north-south direction and different flow patterns are hence expected with different wind directions.

If a typical value of $0.5\,\mathrm{m\,s}^{-1}$ is used for u_*, the timestep is 0.8 s (recalling that the code solves normalised equations where u_* does not need to be specified as input). All simulations are integrated for 50,000 timesteps (excluding spin-up or warm-up time) representing around 11.1 h of physical time to ensure robust statistical convergence, given that turbulent departures are computed with respect to a time average, and higher order statistics are required for the analysis. The campus roughly covers an area of $500 \times 1{,}000$ m, with most building heights between 15 and 20 m.

The focus of our analysis is mainly on qualitative comparisons between the different campus representations. More accurate quantitative comparisons (which are not of great relevance since they are very specific to the canopy being simulated), especially for the complex campus representation, would require a higher grid resolution (see, for example, the discussion in Xie and Castro 2006). Nevertheless, domain size requirements for this study and computational feasibility prevent an increase in the numerical resolution at present. These simulations are using 800,000 grid nodes in each simulation and hence the grid size is comparable to the size used in many recent LES studies. Since a doubling of the spatial resolution (which occurs with a halving of the timestep) requires eight times more floating point operations than the current simulations (16 times if the total physical simulation time is to be preserved), it would not be possible to increase the resolution significantly. One can attempt to increase the resolution without increasing the number of grid points by reducing the domain size; however, when this was tested in the current study, it was detrimental to the quality of the results. When a 200-m high domain was simulated (resulting in a doubling of the vertical resolution), we observed that the flow was spuriously accelerated above the campus due to a severe restriction of the flow cross-section (the top is a zero flow boundary). The blockage effect of the campus on the flow cross-section should be minimized, hence we had to maintain a domain height of 400 m. On the other hand, the horizontal domain (L_x) also cannot be reduced since it is related to the vertical domain size (L_z). One needs to maintain a horizontal domain size at least four times greater than the vertical size (which will be the size of the largest eddies) in a periodic large-eddy simulation of the ABL to allow the eddies to evolve before exiting the domain (see, for example, Moeng et al. 2007). In our simulations, we went just below the limit of this ratio with an $L_x/L_z = 3.75$. In addition, a main objective is to look at the effect of aggregation of the buildings into clusters surrounded by smoother terrain. Hence we need to have an unbuilt area at least equal to that of the campus; this again prevents a reduction in the horizontal size of the domain.

With these limitations on the attainable grid resolution, an assessment of the accuracy of the simulation results is needed to ensure that only the conclusions that can be reliably drawn from this study are addressed. As pointed out earlier, Tseng et al. (2006) showed that a grid resolution of about 6^3 nodes per cube was sufficient for a good match with experimental data using this code. Results with a lower resolution (4^3 nodes) did not match as well with experimental results, but still captured the essential features of the flow. In our study, these

grid resolution requirements are critical for the complex representation of the campus. While most buildings in the complex representation are captured with such a resolution of 4^3 nodes or better, the buildings have very complex shapes and aspect ratios and some details of the buildings are not sufficiently resolved. However, the differences between the three campus representations are extensive and most of these differences span more than 6^3 grid nodes. The differences between the representations are therefore well resolved. As such, despite the relatively low resolution of each building detail, the qualitative comparative analysis is expected to be reliable. Specifically, the results will indicate if the flow simulations are sensitive to the campus representation and will yield an estimate of this sensitivity, despite the fact that this estimate may not be highly accurate. The quantitative details anyway pertain only to this specific urban canopy and are of little general interest. Similarly, later results (see below) reveal the general dynamics of the flow as it moves from the low-roughness terrain to the urban canopy and vice versa.

4 Roughness Length and Drag Coefficient of the Campus

The LES provides normalised velocity profiles (u/u_*) as a function of height; this information can be used to compute the displacement height d and the roughness length of the campus z_0 appearing as parameters in the law-of-the-wall velocity function, which applies under neutral conditions:

$$\frac{u}{u_*} = \frac{1}{\kappa} \ln\left(\frac{z-d}{z_0}\right), \tag{5}$$

where κ is the von Karman constant, u is the average velocity at height z, u_* is the friction velocity at the surface, and d is the displacement height. The velocity profiles used to determine d and z_0 were obtained by averaging the streamwise velocity data from the roof of the highest building on the campus (30 m) up to a height of 50 m. This height range was selected to ensure that the internal boundary layer of the urban canopy is captured. The inflow adjustment zone (see code details above) was omitted from the averaging. Nevertheless, the area around the campus was included since we want to determine the effective z_0 and d for the whole domain, and not just for the built-up areas. The z_0 and d determined from these average profiles will obviously depend on the size of the domain; this is an intentional outcome since the aim is to determine the effective aerodynamic parameters (see Bou-Zeid et al. 2004, 2007) that would be used in a mesoscale model where the whole domain, including the space around the campus, covers one grid cell. The simulated campus is a particular example, and we only analyze its results to answer the questions relating to the campus representation requirements and the effect of wind direction.

In other applications, the aerodynamic properties of the built-up area alone (without surrounding flat surfaces) are of interest. Tests were performed for this study and confirmed that the resulting values of z_0 and d indeed change with the averaging range. However, these tests also indicated that the effects of building representation, which are the focus of this work, on these aerodynamic properties are very similar regardless of the horizontal extent of profile averaging.

An example of the fit for the C–NW simulation is depicted in Fig. 3. A linear trend can be detected in the lower 10% of the ABL (where the law-of-the-wall is expected to hold) down to the level of the highest campus roofs ($\approx$30 m). The values of d and z_0 obtained by the linear fitting for all simulations are listed in Table 1. It is clear from the results that the effect of the campus representation details on the values of z_0 and d is not very significant (about

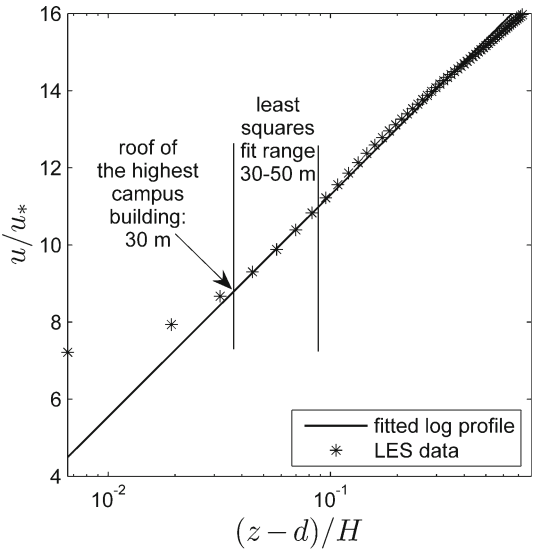

Fig. 3 Least-squares error fit to compute z_0 and d from average velocity profiles

Table 1 Roughness lengths, displacement heights, and drag coefficients for the four simulations

Simulation	z_0 (m)	D (m)	C_d at 30 m
C–NS	0.4356	15.09	0.0256
M–NS	0.4347	15.39	0.026
S–NS	0.4316	15.53	0.026
C–WE	0.4196	14.42	0.0244

1% for z_0 and 3% for d). However, the trend is such that increasing building complexity increases z_0 and reduces d; the combination of these two effects indicates that the higher complexity campus representation produces a smoother velocity profile and lower shear at the top of the canopy.

To compare the actual effect of the campus representation on the drag we compute the drag coefficient C_d as a function of height for neutral conditions:

$$C_d = 2\frac{\tau_s}{\rho u^2} = 2\frac{u_*^2}{u^2} = 2\left(\frac{\kappa}{\ln[(z-d)/z_0]}\right)^2, \tag{6}$$

where τ_s is the surface stress. This height-dependent form of the drag coefficient is frequently used in ABL and urban flow applications (Cheng and Castro 2002; Coceal and Belcher 2004). A unique, height-independent, drag coefficient cannot be formulated for such applications since a unique reference velocity cannot be defined here (similar, for example, to U_∞ used in studying drag coefficients over a cylinder or a flat plate in an infinite fluid). The values of C_d at a height of 30 m are reported in Table 1 and the profiles of C_d up to a height of 80 m are depicted in Fig. 4. The values of C_d decrease with height as expected. Note the small differences in the C_d profiles for the different campus representations when the wind is from the north (NS simulations). This strongly suggests that the difference in the level of detail of the campus representation does not produce a significant difference in the flow at the campus scale (same drag). The conclusion that the details of the campus representation are not relevant for the results when viewed at the campus scale (i.e. when the aggregate atmosphere-campus exchanges are needed) is a new finding of significant relevance. However,

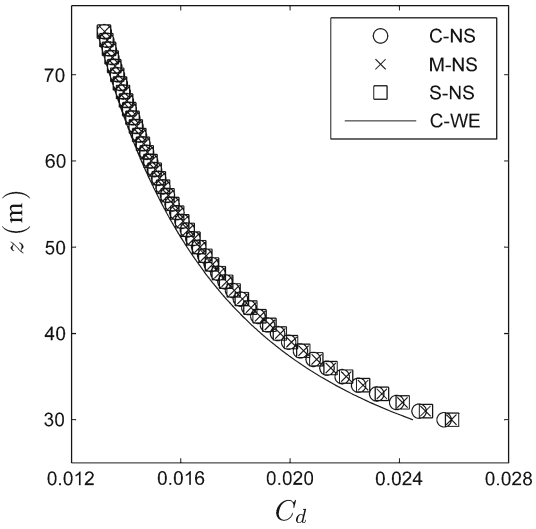

Fig. 4 Profile of the drag coefficient as a function of height for the different simulations

this result is not entirely surprising considering that the drag of the campus is mainly a form drag (as concluded also by Xie and Castro 2006) that is insensitive to the representation details and more sensitive to the blockage effect of the campus. This blockage effect is about the same for the three representations since, as noted above, their projected surface areas perpendicular to the wind direction are about the same. The slightly lower form drag of the more "porous" complex representation is probably offset by the slightly higher shear drag due to the additional wall area in that complex representation. These results suggest that urban area parameterisations (in mesoscale or larger scale models) do not need to account for all the details of the buildings or even to consider the smaller buildings in the first place, if the different representations maintain a realistic frontal projected area.

On the other hand, the effect of wind direction is more significant. The C–WE simulation has a lower d and a lower z_0, resulting in a lower C_d (by about 5%) as can be seen in Fig. 4 and the last column of Table 1. This indicates that the campus exerts a lower drag when the wind is from the west. This can be attributed to the campus alignment along the west-east direction; the campus will therefore exert a lower blockage effect and a lower drag when the wind is from that direction (this simple explanation works only for configurations such as the one simulated here where the buildings are rather tightly packed). While these last results are very specific to the building configurations studied here and are probably irrelevant to other urban flow studies, they illustrate that the flow and the aggregate momentum exchange are not insensitive to the wind direction. In fact, when the drag is computed for the campus only (without the surrounding flat area, results not shown here), the effect of the wind direction is even more pronounced. This underscores the complexity of parameterizing built-up areas in coarse meteorological models and the importance of taking wind direction and/or meandering (relative to building configuration) into account. This dependence on the wind direction is indirectly accounted for in models that parameterize d and z_0 for urban areas in terms of the "λ parameters" (see Britter and Hanna (2003) or Grimmond and Oke (1999) for details): $\lambda_p = A_p/A_T$ and $\lambda_f = A_f/A_T$, where A_p is the total building plan area (surface covered by buildings when seen from above), A_f is the total building frontal area (sum of building surfaces facing the mean wind direction), and A_T is the total surface area (the total land area of the urban zone). The wind direction will of course influence A_f. In that regard,

a thorough testing of the "λ parameters" models for random building configurations and for wind directions that are not perpendicular to the faces of the buildings is needed and can be performed using LES simulations as a benchmark.

5 Flow Adjustments Upstream, Over, and Downstream of the Campus

5.1 Mean Velocity Profiles

As air flows over the campus, both the mean flow and the turbulence are distorted by the interaction with the buildings. In this section, we study this interaction for the north-south flow simulations since it is the only direction that allows us to clearly divide the domain into upwind, over-the-campus, and downwind regions. We also omit the results from the medium complexity campus representation for clarity of presentation, but we verified that they invariably lie between the results of the simplest and most complex representations that are presented here.

We start by analyzing the profiles of streamwise and vertical mean velocities upstream, over, and downstream of the campus; the averages are taken over fluid grid cells only, i.e. the zero fluid velocities in the buildings are not considered. In addition, we subtract the mean vertical profile of the velocities averaged over the whole domain to remove the strong mean vertical trends and emphasize the effect of the campus. These deviations from the mean profiles are depicted in Fig. 5. The streamwise velocity over the campus is reduced significantly below the top of the buildings ($z/H < 0.1$) (Fig. 5a), it increases behind the campus, and at a height of about twice the building heights ($z/H = 0.2$), it almost recovers its upstream profile. Note also the higher velocity at elevations of $z/H > 0.1$ over the campus. This speed-up above the buildings is of course expected and compensates for the reduced velocity inside the canopy as the atmospheric flow is diverted over the campus. The effect of this flow diversion over the campus is very clearly illustrated in the vertical velocity profiles of Fig. 5b. Upstream from, and over, the campus, the flow is diverted upwards producing positive vertical velocity profiles. A subsidence (negative vertical velocity) region is found behind the campus where the streamwise flow near the surface accelerates again, drawing air from above. It is interesting to note that in the upstream region, the flow is diverted downwards below the campus top and upwards above the campus top.

For the streamwise velocity profiles in Fig. 5a, the effect of the campus representation details is minimal. On the other hand, the variations due to campus representation are more pronounced in the vertical velocities of Fig. 5b. This can be explained by the fact that the streamwise velocity profiles are strongly affected by the campus drag, which produces significant departures from the domain mean (maximum difference of $1.3\,\mathrm{m\,s^{-1}}$) and the discrepancies due to the campus representation (root-mean-square (rms) difference $\approx 0.048\,\mathrm{m\,s^{-1}}$) are small in comparison. On the other hand, for vertical velocities, the campus produces maximum departures from the domain mean of about $0.12\,\mathrm{m\,s^{-1}}$ and the discrepancies due to the campus representation (rms difference $\approx 0.0073\,\mathrm{m\,s^{-1}}$) are relatively more significant.

The simple campus representation produces the largest upward flow deviation upstream of the campus; while with the complex representation, (more porous canopy and more distributed buildings) upwards flow deviation is more evenly divided between the upstream and over-the-campus zones. These results suggest that the effect of the campus representation complexity on the local simulated velocity profiles, while still small, is more important than its effect on the profiles averaged over the whole domain (previous section). Obviously,

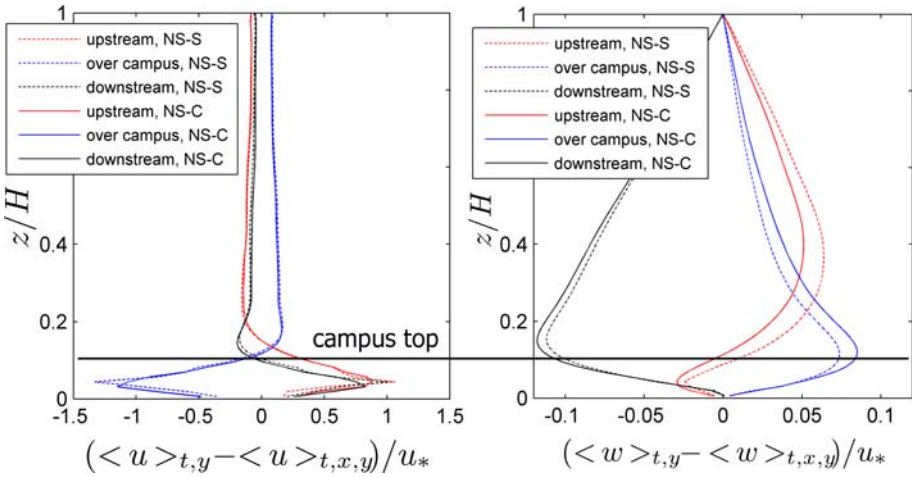

Fig. 5 Deviation of the vertical profiles of u and w from the domain mean upstream, over, and downstream of the campus for the simple (*dashed lines*) and complex (*solid lines*) building representations and north-south flow

at the street level where the details of the flow in the canopy are of interest, the level of detail of the buildings is very important (Xie and Castro 2006).

5.2 Root-Mean Square (rms) Velocities and Turbulent Kinetic Energy

The rms velocities in the streamwise (u_{rms}) and vertical (w_{rms}) directions are depicted in Fig. 6, noting once again that the rms values were computed with respect to a time average. Upstream of the campus, the two profiles are "smooth" and almost no differences can be noted between the simple and complex campus representations, as expected. Over the campus, the rms values slightly decrease compared to upstream values for both u_{rms} and w_{rms}. The simple campus representation gives a significantly higher value below and close to the campus top (about 20% higher than the complex campus representation). This suggests that the large structures in the simple representation produce a higher intensity of turbulence than the more numerous but smaller structures in the complex campus representation. Downstream, the turbulence increases again close to the canopy top. Note that for u_{rms}, the peaks in the profiles over and downstream of the campus occur at $z/H \approx 0.1$, i.e. at the top of the canopy while the upstream peak occurs at a lower height.

The effect of the buildings on the streamwise velocity rms extends only to a height of $z/H \approx 0.3$. As for the mean velocity, the effect on the vertical velocity component is more pronounced and extends much higher, almost to the top of the domain. This again is due to the fact that the perturbation to the flow due to the campus in the vertical direction is significant compared to the "baseline" vertical variation of that component. In the streamwise direction, the vertical profiles are significantly influenced by the drag at the surface and the perturbations due to the campus are relatively less important. Also note the ratio of $u_{\mathrm{rms}}/w_{\mathrm{rms}} > 1$ at all heights indicating, as expected in wall bounded flow, a high degree of anisotropy of turbulence especially near the wall.

The profiles in Fig. 6 suggest that the turbulence levels are almost the same upstream, over and downstream of the campus. This is, of course, a simple picture that does not account for

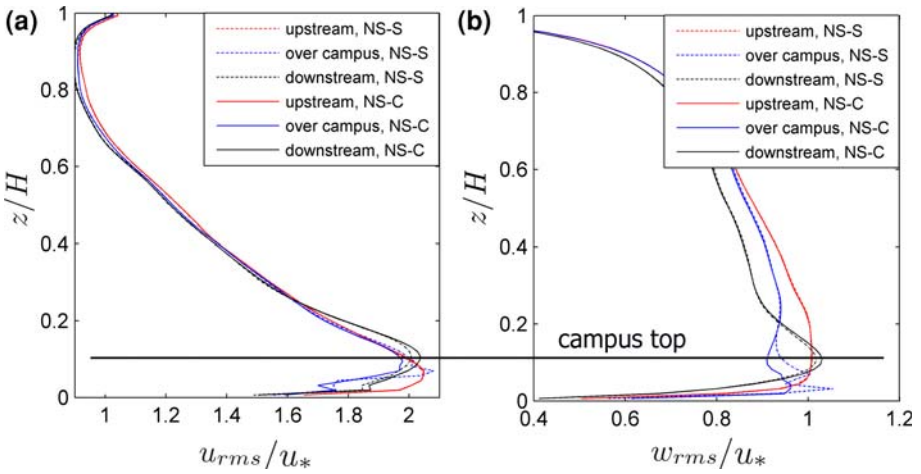

Fig. 6 Normalised u and w rms velocities upstream, over, and downstream of the campus for the simple (*dashed lines*) and complex (*solid lines*) building representations with north-south winds

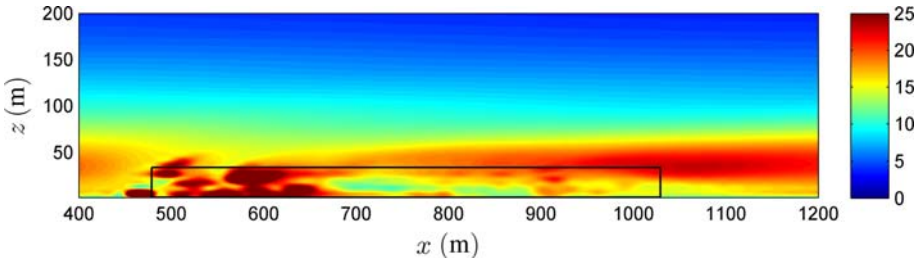

Fig. 7 x–z slice with TKE/u_*^2 levels for simulation C–NS, averaged in time (over 11.1 h) and in the cross-stream direction; *black rectangle* delineates the extent of the campus

the rapid variation of the turbulent kinetic energy (TKE) over the campus. Figure 7 shows an x–z slice with the TKE values averaged in time and in the cross-stream (y) direction over and around the campus (which extends from 475 to 1,050 m in the x direction and up to 30 m in the z direction; the edges of the campus are delineated by the black rectangle in the figure). The contours are patchy due to cross-stream averaging over the non-uniform building distributions. Note the very high TKE at the upstream edge of the campus (500 to 650 m) and the significant reduction in the TKE as the flow velocity is reduced, and as the campus drag and TKE cascade to the subgrid scales increase further downstream. Behind the campus ($x > 1{,}000$ m), a smooth zone of high TKE is observed in the shear layer at the height corresponding to building tops; the high TKE here is due to strong shear production as will be illustrated later.

6 Stresses

Figure 8 depicts the resolved, SGS, and total Reynolds stresses (sum of resolved and SGS) for the complex representation (the other representations, as expected, gave similar trends subject to the quantitative differences discussed in the previous sections). The resolved stresses

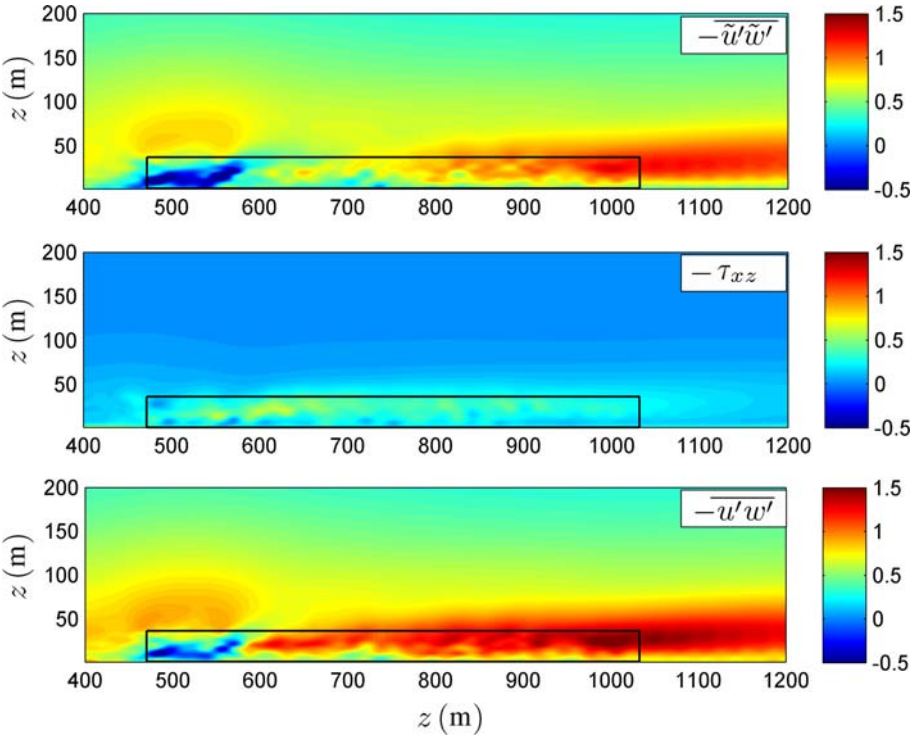

Fig. 8 Resolved stress (*top*), SGS stress (*middle*), and total Reynolds stress, cross-stream and time-averaged over the campus (all normalised by u_*^2)

are significantly larger than their SGS counterparts almost throughout the domain. However, the single region where the SGS contribution to the total stresses is important is in the direct vicinity of the buildings. The flow dynamics in this zone are of course very important and having to rely on the SGS model to compute a significant part of the total stress is inconvenient. However, the LES technique cannot avoid this problem if flows with a realistic Reynolds number ($\sim 10^8$ in the ABL) are to be simulated (precluding LES with near-wall resolution, see Pope 2000). Improved grid resolution in urban areas (through grid refinement or increases in computational resources) reduces the SGS contribution in the urban canopy and increases the range of the resolved scales; this should have a positive effect on the quality of large-eddy simulations (Cheng and Castro 2002; Tseng et al. 2006). Note that over flat homogeneous surfaces, LES results should converge beyond a given resolution if the grid size is in the inertial subrange. For simulations with complex geometries on the other hand, the geometry of the problem (rather than the limits of the inertial subrange) may in many cases dictate the requirements on the grid resolution.

Another very interesting feature in Fig. 8 is the zone of negative stresses that indicates an upward transfer of momentum close to the surface, between $x \approx 475$ and 575 m, above which is a zone of strong positive stresses (downward momentum transfer). This indicates that a very strong momentum sink exists in this zone at a height of 20–30 m; this zone corresponds to the building canopy top at the upstream edge of the campus. In that region, we find that a very strong shear (du/dz) exists (much higher than du/dz at the surface) since the flow above the campus has not yet adjusted to the roughness of the campus while the flow inside the campus has decelerated. Further downstream, the flow above and inside the campus

adjusts to the new surface, the shear is reduced, and the downwards momentum transfer is more evenly distributed across the depth of the canopy. Towards the downstream edge of the campus (after 800 m), the building density is reduced (see Fig. 2) and the flow accelerates again; strong downward momentum transfer is again observed as the ground becomes the main momentum sink.

The causes of this upward transfer of momentum at the leading edge are not the same as for the upward transfer observed in forests (Lee and Black 1993), where the flow near the surface (through the tree stems) has a higher velocity than the flow above (through the tree crowns) (Shaw 1977). In that case, the crowns act as a momentum sink and momentum is transferred from the stem zone to the crown zone possibly throughout the canopy. In our study, the upward transfer is limited to the upstream edge of the campus. This local upward momentum transfer in building canopies is observed if the buildings are clustered into small "neighbourhoods" with low roughness areas in between. The effect of this horizontal variability (acceleration and deceleration of the flow) on the dynamics of the atmospheric flow and on land-atmosphere exchanges in built-up areas has not been adequately studied to date.

7 TKE Budget over the Campus

The mean (overbar) resolved (tilde) turbulent kinetic energy ($\overline{\tilde{e}}$) equation can be written as:

$$\frac{\partial \overline{\tilde{e}}}{\partial t} + \overline{\tilde{u}}_j \frac{\partial \overline{\tilde{e}}}{\partial x_j} = -\overline{\tilde{u}_i' \tilde{u}_j'} \frac{\partial \overline{\tilde{u}_i}}{\partial x_j} - \frac{\partial \overline{\tilde{u}_j' \tilde{e}}}{\partial x_j} - \frac{1}{\rho} \frac{\partial \overline{\tilde{u}_j' \tilde{p}'}}{\partial x_j} - \frac{\partial \overline{\tilde{u}_i' \tau_{ij}'}}{\partial x_j} + \overline{\tau_{ij}' \tilde{S}_{ij}'} + \overline{f_i' \tilde{u}_i'}, \tag{7}$$

where the overbar denotes Reynolds averaging, and was taken as the temporal mean over the whole simulation in our analysis since spatial means are not well defined in complex domains (no spatial direction with homogeneous turbulence statistics). The prime denotes the turbulent component of the variable, and all other variables are as defined previously. The equation omits the buoyancy production or destruction term, which is not relevant for neutral flows, as well as the viscous dissipation, which is not significant at the scales resolved in LES with wall modelling. In our simulations, the unsteady term ($\partial/\partial t$) can be neglected since steady state conditions are established. The two terms on the left represent the material derivative of $\overline{\tilde{e}}$. The first term on the right is the shear production or destruction, the second term is the turbulent transport, the third is the pressure transport, the fourth is the SGS transport, and the fifth is the "SGS dissipation", i.e. the flux of TKE from the resolved to the subgrid scales. The last term is a sink of resolved TKE due to the force exerted by the buildings on the flow, f_i.

We focus our attention on the shear production and SGS dissipation of TKE. Figure 9 shows the time-averaged and cross-stream-averaged SGS dissipation, and as expected, SGS

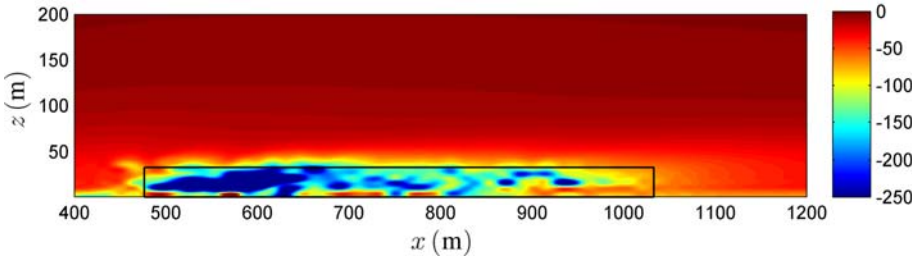

Fig. 9 SGS dissipation (normalised), cross-stream and time-averaged, over the campus

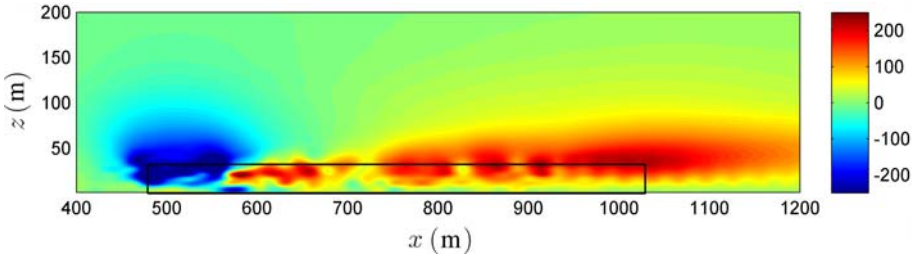

Fig. 10 Normalised shear production, cross-stream and time averaged, over the campus

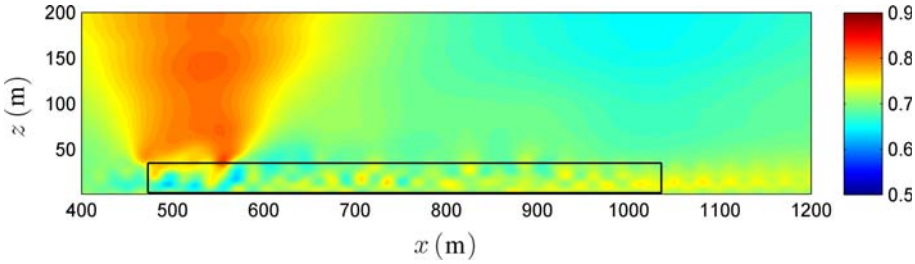

Fig. 11 Alignment (cosine of the angle) between the mean velocity vector and the eigenvector of the resolved strain rate tensor corresponding to the largest eigenvalue (stretching eigenvalue)

dissipation is large inside the canopy; this is probably due to two factors: (i) strong shear inside the canopy increases the production of TKE (see below), which has to be partially balanced by higher dissipation, and (ii) this TKE production is mostly at small scales (on the order of the street canyon size, i.e. slightly larger than the grid scale) that have shorter turnover times and rapidly transfer their energy to the (spectrally close) smaller subgrid scales.

Figure 10 depicts the shear production term; as explained above, this production is high inside the building canopy. The contours are again patchy due to the cross-stream averaging over the non-uniform building distribution; however, a uniform area of very high production can be noted at the downstream edge of the campus. The striking feature in Fig. 10 is the relatively large area of global backscatter (negative shear production) indicating that the kinetic energy is being transferred from the turbulent motions to the mean flow. Global backscatter is not common and very particular flow conditions are needed to produce this transfer of energy (see Liberzon et al. 2005 and Chen et al. 2006).

Liberzon et al. (2005) studied the occurrence of negative TKE production in a buoyant flow (Rayleigh–Bénard convection) and in a mechanical agitated neutral shear flow. They concluded that regions of negative shear production occur where the mean velocity vector $\bar{u}$ is noticeably aligned with the first eigenvector of the strain rate tensor $S_{ij} = 0.5\left(\partial u_i/\partial x_j + \partial u_j/\partial x_i\right)$ (corresponding to the largest positive eigenvalue, i.e. to stretching motions). We checked this alignment (the cosine of the angle of the velocity vector and the first eigenvector of the resolved part of the strain rate tensor) and plotted the results in Fig. 11. Higher values of the cosine indicate a better alignment. Indeed we make the same observation as Liberzon et al. (2005) and note the strong alignment in the same region ($475\,\mathrm{m} < x < 575\,\mathrm{m}$). However, we also observe that, while strong global backscatter seems to start at a height of about 10 m in that area, the alignment is not very strong until a height of 25 m is reached. In any case, this observation does not explain what flow conditions tend to favour such an alignment and the backscatter of energy to the mean flow.

Chen et al. (2006) also observed global backscatter in experiments of a rapid cycle of straining and destraining and attributed the backscatter in their experiments to "a mismatch between the orientation of straining and the magnitude of Reynolds stresses generated by prior processes". The mean resolved strain rate ($\partial\overline{\tilde{u}_i}/\partial x_j$) adjusts more rapidly than the resolved Reynolds-stress tensor ($-\overline{\tilde{u}_i'\tilde{u}_j'}$), causing such a mismatch when the flow undergoes sudden distortions. Therefore, in zones where such a mismatch occurs, the flow geometry might allow global backscatter. The upstream edge of the campus is certainly characterised by strong streamwise and vertical variations and in that area the strain adjusts very rapidly. The stress however, as depicted in Fig. 8, only starts adjusting after $x \approx 575$ m, which corresponds very well to the area where the shear production becomes positive again. Also note that the zone of global backscatter (Fig. 10) extends beyond the zone of upwards momentum transfer (lower part of Fig. 8). Instead, the global backscatter zone matches with the whole region where the stresses are strong and are continuing to adjust to the new building roughness, hence supporting the explanation of Chen et al. (2006).

Forward scatter is understood to be mainly caused by the stretching of vortices by the strain rate, leading to a cascade of energy to smaller scales. Backscatter, on the other hand, is due to the compression of these vortices by the strain rate in the fluid. At the leading edge of the campus, the strain rate adjusts to the new flow geometry rapidly while the stresses and vortices are still representative of upstream conditions. When the mismatch leads to compression of these vortices and to the final transfer of their energy to the mean flow, backscatter is observed. However, further detailed analysis is required to fully understand the flow dynamics leading to this global backscatter at the leading edge of the campus.

8 Summary and Conclusion

Four large-eddy simulations of neutral ABL flow over a built-up area were performed with the aim of determining the effect of building representation detail on atmospheric flow and its adjustment as it passes from flat to built-up surfaces and vice versa. Three simulations had the same wind direction but varying level of building details included in the modelling domain. The fourth simulation had a well-detailed building representation but a different wind direction.

For each simulation, the average drag, effective roughness, and displacement height were computed illustrating how high resolution local simulations can be performed to compute aerodynamic parameters that can be subsequently used to parameterize a building canopy in coarser models. The different wind directions had a non-negligible impact on the results (C_d, z_o and d) due to the preferential north-south orientation of the individual buildings and the preferential west-east orientation of the building cluster studied here. Consequently, the meandering of the mean wind will also have an effect on the drag exerted by the canopy and should be considered as well in parameterisations of urban areas.

On the other hand, the campus representations of increasing complexity yielded very similar results. The small-scale details of the canopy did not seem to affect the mean flow and aerodynamic parameters significantly, implying that a high level of detail in representing the canopy in local models is not needed if the aim is to upscale the results to coarser models. This also indicates that the urban canopy models (for example, models based on the λ parameters) do not require highly detailed morphometric data to yield realistic results and that such model formulations should not be sensitive to the small morphometric details in the first place. The relevant parameter is the projected frontal area, which directly leads to

flow blockage and form drag. Our different models of the urban canopy were constructed to have very similar projected frontal areas, and our conclusions are therefore only confirmed under such conditions.

The mean velocity profiles upstream, over, and downstream of the building cluster for the different simulations were also analyzed and indicated moderate differences between the simulations with different campus representations. For the turbulent components, however, the effect of the different campus representations was more important, with differences between the campus models reaching up to 20 percent. The vertical components of both the mean and turbulent velocities were found to be more sensitive to the campus representation than the streamwise components. Analysis of the stresses indicates that the subgrid-scale part is important in and close to the campus.

This suggests that inclusion of a high level of detail in a building representation remains important in local models if the aim is to simulate the flow and the transport of pollutants at the street or canopy scale. For such simulations, the highest attainable grid resolution should be used all through the urban canopy (not just over the buildings). This will have a positive effect on the grid resolution of the buildings and at the same time will reduce the modelled SGS fraction of the turbulent stresses, allowing more turbulent scales to be directly resolved. However, morphometric data might often be available at a resolution that cannot be captured in the local simulation due to grid resolution restrictions. In such instances, regardless of the aim of the simulation (upscaling or local flow dynamics), we recommend constructing the simplified version of the canopy so as to have the same λ parameters as the high-detail morphometric data.

This study also investigated the flow adjustment from a flat/vegetated to a built-up area and back to a flat/vegetated area. The TKE was shown to be very high at the upstream edge of the campus and to decrease very rapidly as the air flows through the building canopy, only to increase again downstream from the campus. The shear production and dissipation of the TKE were also analyzed and a region with strong "global backscatter" was observed at the upstream edge of the campus, indicating a transfer of energy from the turbulence to the mean flow. The global backscatter can be attributed to a mismatch (imbalance) of the strain and the stress in the flow that occurs when sudden perturbations are imposed. This, along with the strong variations in the velocities, stresses, and TKE as the air flows over the building cluster, underlines the importance of including surface variability in urban canopy models.

At present, most urban canopy models are based exclusively on the properties of the canopy and exclude the effect of the surroundings; therefore, the effects of these strong streamwise flow variations are not included in these models. These variations, and hence the horizontal spatial scale of the urban canopy, will have an important effect on the canopy-atmosphere exchange rates, just as with variable natural terrain (Bou-Zeid et al. 2007). Therefore, a heterogeneous suburban canopy cannot be adequately parameterised without consideration of its subgrid spatial variability, relative to the grids of regional or global atmospheric models.

Acknowledgements The authors would like the thank the Swiss National Science Foundation for its supports for this work through grant number 200021-107910 and through the National Competence Centre in Research on Mobile Information and Communication Systems (NCCR-MICS) under grant number 5005-67322. Professor Bou-Zeid was also supported by the High Meadows Sustainability Fund through the "Sensor Network over Princeton" project. The authors are also grateful to the Swiss National Supercomputing Centre for its support and allocation of ample computing resources for the simulations of this paper. Professor Charles Meneveau's and Professor Yu-Heng Tseng's contributions to the development of the code and to the implementation of the immersed boundary method are also greatly appreciated.

References

Albertson JD, Parlange MB (1999a) Natural integration of scalar fluxes from complex terrain. Adv Water Resour 23(3):239–252

Albertson JD, Parlange MB (1999b) Surface length scales and shear stress: implications for land–atmosphere interaction over complex terrain. Water Resour Res 35(7):2121–2132

Albertson JD, Kustas WP, Scanlon TM (2001) Large-eddy simulation over heterogeneous terrain with remotely sensed land surface conditions. Water Resour Res 37(7):1939–1953

Avissar R (1995) Recent advances in the representation of land–atmosphere interactions in general-circulation models. Rev Geophys 33:1005–1010

Belcher SE, Jerram N, Hunt JCR (2003) Adjustment of a turbulent boundary layer to a canopy of roughness elements. J Fluid Mech 488:369–398

Bou-Zeid E, Meneveau C, Parlange MB (2004) Large-eddy simulation of neutral atmospheric boundary layer flow over heterogeneous surfaces: blending height and effective surface roughness. Water Resour Res 40(2):W02505. doi:10.1029/2003WR002475

Bou-Zeid E, Meneveau C, Parlange MB (2005) A scale-dependent Lagrangian dynamic model for large eddy simulation of complex turbulent flows. Phys Fluids 17(2):025105. doi:10.1063/1.1839152

Bou-Zeid E, Parlange MB, Meneveau C (2007) On the parameterization of surface roughness at regional scales. J Atmos Sci 64(1):216–227. doi:10.1175/JAS3826.1

Bou-Zeid E, Vercauteren N, Parlange MB, Meneveau C (2008) Scale dependence of subgrid-scale model coefficients: an a priori study. Phys Fluids 20(11):115106

Bradbrook KF, Lane SN, Richards KS, Biron PM, Roy AG (2000) Large eddy simulation of periodic flow characteristics at river channel confluences. J Hydraul Res 38(3):207–215

Britter RE, Hanna SR (2003) Flow and dispersion in urban areas. Annu Rev Fluid Mech 35:469–496

Brutsaert W (1998) Land-surface water vapor and sensible heat flux: spatial variability, homogeneity, and measurement scales. Water Resour Res 34(10):2433–2442. doi:10.1029/98WR01340

Cai XM (1999) Large-eddy simulation of the convective boundary layer over an idealized patchy urban surface. Q J Roy Meteorol Soc 125(556):1427–1444

Calhoun R, Gouveia F, Shinn J, Chan S, Stevens D, Lee R, Leone J (2005) Flow around a complex building: experimental and large-eddy simulation comparisons. J Appl Meteorol 44(5):571–590

Celani A (2007) The frontiers of computing in turbulence: challenges and perspectives. J Turbul 8(1):1–9

Chen J, Meneveau C, Katz J (2006) Scale interactions of turbulence subjected to a straining–relaxation–destraining cycle. J Fluid Mech 562:123–150

Cheng H, Castro IP (2002) Near wall flow over urban-like roughness. Boundary-Layer Meteorol 104(2):229–259

Coceal O, Belcher SE (2004) A canopy model of mean winds through urban areas. Q J Roy Meteorol Soc 130(599):1349–1372

Dupont S, Mestayer PG (2006) Parameterization of the urban energy budget with the submesoscale soil model. J Appl Meteorol Clim 45(12):1744–1765

Eliasson I, Offerle B, Grimmond CSB, Lindqvist S (2006) Wind fields and turbulence statistics in an urban street canyon. Atmos Environ 40(1):1–16

Emeis S (2004a) Parameterization of turbulent viscosity over orography. Meteorol Z 13(1):33–38

Emeis S (2004b) Vertical wind profiles over an urban area. Meteorol Z 13(5):353–359

Emeis S, Turk M (2004) Frequency distributions of the mixing height over an urban area from SODAR data. Meteorol Z 13(5):361–367

Germano M, Piomelli U, Moin P, Cabot WH (1991) A dynamic subgrid-scale eddy viscosity model. Phys Fluids A 3(7):1760–1765

Grimmond CSB, Oke TR (1999) Aerodynamic properties of urban areas derived, from analysis of surface form. J Appl Meteorol 38(9):1262–1292

Grimmond CSB, King TS, Roth M, Oke TR (1998) Aerodynamic roughness of urban areas derived from wind observations. Boundary-Layer Meteorol 89(1):1–24

Harman IN, Belcher SE (2006) The surface energy balance and boundary layer over urban street canyons. Q J Roy Meteorol Soc 132(621):2749–2768

Kanda M, Moriwaki R, Kasamatsu F (2004) Large-eddy simulation of turbulent organized structures within and above explicitly resolved cube arrays. Boundary-Layer Meteorol 112(2):343–368

Keylock CJ, Hardy RJ, Parsons DR, Ferguson RI, Lane SN, Richards KS (2005) The theoretical foundations and potential for large-eddy simulation (LES) in fluvial geomorphic and sedimentological research. Earth Sci Rev 71(3–4):271–304

Kleissl J, Kumar V, Meneveau C, Parlange MB (2006) Numerical study of dynamic Smagorinsky models in large-eddy simulation of the atmospheric boundary layer: validation in stable and unstable conditions. Water Resour Res 42(6):W06D10. doi:10.1029/2005WR004685

Kumar V, Kleissl J, Meneveau C, Parlange MB (2006) Large-eddy simulation of a diurnal cycle of the atmospheric boundary layer: atmospheric stability and scaling issues. Water Resour Res 42(6):W06D09. doi:10.1029/2005WR004651

Lee XH, Black TA (1993) Atmospheric-turbulence within and above a Douglas–Fir stand. 1. Statistical properties of the velocity-field. Boundary-Layer Meteorol 64(1-2):149–174

Liberzon A, Luthi B, Guala M, Kinzelbach W, Tsinober A (2005) Experimental study of the structure of flow regions with negative turbulent kinetic energy production in confined three-dimensional shear flows with and without buoyancy. Phys Fluids 17(9):095110

Lilly DK (1967) The representation of small scale turbulence in numerical simulation experiments. In: IBM scientific computing symposium on environmental sciences, White Plains, New York, pp 195–209

Lin CL, Glendening JW (2002) Large eddy simulation of an inhomogeneous atmospheric boundary layer under neutral conditions. J Atmos Sci 59(16):2479–2497

Lyn DA, Rodi W (1994) The flapping shear-layer formed by flow separation from the forward corner of a square cylinder. J Fluid Mech 267:353–376

Masson V (2000) A physically-based scheme for the urban energy budget in atmospheric models. Boundary-Layer Meteorol 94(3):357–397

Meinders ER, Hanjalic K (1999) Vortex structure and heat transfer in turbulent flow over a wall-mounted matrix of cubes. Int J Heat Fluid Flow 20(3):255–267

Meinders ER, Hanjalic K (2002) Experimental study of the convective heat transfer from in-line and staggered configurations of two wall-mounted cubes. Int J Heat Mass Transf 45(3):465–482

Meneveau C, Katz J (2000) Scale-invariance and turbulence models for large-eddy simulation. Annu Rev Fluid Mech 32:1–32

Meneveau C, Lund TS, Cabot WH (1996) A Lagrangian dynamic subgrid-scale model of turbulence. J Fluid Mech 319:353–385

Moeng CH, Dudhia J, Klemp J, Sullivan P (2007) Examining two-way grid nesting for large eddy simulation of the PBL using the WRF model. Mon Weather Rev 135(6):2295–2311

Molod A, Salmun H, Waugh DW (2003) A new look at modeling surface heterogeneity: extending its influence in the vertical. J Hydrometeorol 4(5):810–825

Monin AS, Obukhov AM (1954) Basic laws of turbulent mixing in the ground layer of the atmosphere (in Russian), vol 151. Trudy Geofizicheskogo Instituta, Akademiya Nauk SSSR, pp 163–187

Orszag SA, Pao YH (1974) Numerical computation of turbulent shear flows. Adv Geophys 18(A):224–236

Parlange MB, Brutsaert W (1993) Regional shear-stress of broken forest from radiosonde wind profiles in the unstable surface-layer. Boundary-Layer Meteorol 64(4):355–368

Piomelli U (1999) Large-eddy simulation: achievements and challenges. Prog Aerosp Sci 35(4):335–362

Pope SB (2000) Turbulent flows. Cambridge University Press, Cambridge, 771 pp

Porte-Agel F, Meneveau C, Parlange MB (2000) A scale-dependent dynamic model for large-eddy simulation: application to a neutral atmospheric boundary layer. J Fluid Mech 415:261–284

Roberts SM, Oke TR, Grimmond CSB, Voogt JA (2006) Comparison of four methods to estimate urban heat storage. J Appl Meteorol Clim 45(12):1766–1781

Rotach MW, Fisher B, Piringer M (2002) COST 715 workshop on urban boundary layer parameterizations. Bull Am Meteorol Soc 83(10):1501–1504

Roth M (2000) Review of atmospheric turbulence over cities. Q J Roy Meteorol Soc 126(564):941–990

Roth M, Salmond JA, Satyanarayana ANV (2006) Methodological considerations regarding the measurement of turbulent fluxes in the urban roughness sublayer: the role of scintillometery. Boundary-Layer Meteorol 121(2):351–375

Roulet YA, Martilli A, Rotach MW, Clappier A (2005) Validation of an urban surface exchange parameterization for mesoscale models—1D case in a street canyon. J Appl Meteorol 44(9):1484–1498

Sagaut P (2003) Large eddy simulation for incompressible flows. Springer, Berlin, 426 pp

Shaw RH (1977) Secondary wind speed maxima inside plant canopies. J Appl Meteorol 16(5):514–521

Shen L, Yue DKP (2001) Large-eddy simulation of free-surface turbulence. J Fluid Mech 440:75–116

Smagorinsky J (1963) General circulation experiments with the primitive equations: I. the basic experiment. Mon Weather Rev 91:99–164

Stoll R, Porte-Agel F (2006) Dynamic subgrid-scale models for momentum and scalar fluxes in large-eddy simulations of neutrally stratified atmospheric boundary layers over heterogeneous terrain. Water Resour Res 42(1):W01409

Tominaga Y, Mochida A, Murakami S, Sawaki S (2008) Comparison of various revised k-[epsilon] models and LES applied to flow around a high-rise building model with 1:1:2 shape placed within the surface boundary layer. J Wind Eng Ind Aerodyn 96(4):389–411

Tseng YH, Meneveau C, Parlange MB (2006) Modeling flow around bluff bodies and predicting urban dispersion using large eddy simulation. Environ Sci Technol 40(8):2653–2662

Wood N (2000) Wind flow over complex terrain: a historical perspective and the prospect for large-eddy modelling. Boundary-Layer Meteorol 96(1-2):11–32

Xie ZT, Castro IP (2006) LES and RANS for turbulent flow over arrays of wall-mounted obstacles. Flow Turbul Combust 76(3):291–312

Xie ZT, Li JC (2005) A numerical study for turbulent flow and thermal influence over inhomogenous canopy of roughness elements. Environ Fluid Mech 5(6):577–597

Yue WS, Meneveau C, Parlange MB, Zhu WH, van Hout R, Katz J (2007a) A comparative quadrant analysis of turbulence in a plant canopy. Water Resour Res 43(5):W05422. doi:10.1029/2006WR005583

Yue WS, Parlange MB, Meneveau C, Zhu WH, van Hout R, Katz J (2007b) Large-eddy simulation of plant canopy flows using plant-scale representation. Boundary-Layer Meteorol 124(2):183–203

Zhang N, Jiang WM, Miao SG (2006) A large eddy simulation on the effect of buildings on urban flows. Wind Struct 9(1):23–35